

CAUGHT IN THE ACT: THE ONSET OF MASSIVE STAR FORMATION

H. BEUTHER¹, T.K. SRIDHARAN¹, M. SAITO²
hbeuther@cfa.harvard.edu, tksridha@cfa.harvard.edu, Masao.Saito@nao.ac.jp
Draft version from November 19, 2018, accepted for ApJL

ABSTRACT

Combining mid-infrared data from the SPITZER Space Telescope with cold gas and dust emission observations from the Plateau de Bure Interferometer, we characterize the Infrared Dark Cloud IRDC 18223-3 at high spatial resolution. The millimeter continuum data reveal a massive $\sim 184 M_{\odot}$ gas core with a projected size of ~ 28000 AU that has no associated protostellar mid-infrared counterpart. However, the detection of $4.5 \mu\text{m}$ emission at the edge of the core indicates early outflow activity, which is supported by broad CO and CS spectral line-wing emission. Moreover, systematically increasing $\text{N}_2\text{H}^+(1-0)$ line-width toward the mm core center can be interpreted as additional evidence for early star formation. Furthermore, the $\text{N}_2\text{H}^+(1-0)$ line emission reveals a less massive secondary core which could be in an evolutionary stage prior to any star formation activity.

Subject headings: stars: formation – stars: individual (IRDC 18223-3) – stars: winds, outflows – stars: early-type

1. INTRODUCTION

Massive star formation research has focused so far on evolutionary stages either observable in the cm regime due to free-free emission (Ultracompact HII regions, e.g., Kurtz et al. 2000; Churchwell 2002), or on slightly younger stages which emit in the (sub)mm bands and are also detectable at mid-infrared (MIR) wavelengths due to warm dust emission (e.g., Molinari et al. 1996; Sridharan et al. 2002). The initial phase prior to any cm free-free and MIR warm dust emission was observationally largely inaccessible. The most basic identification criterion for the initial stages of massive star formation is that such regions have to be bright in the (sub)mm regime due to cold dust and gas, and weak or undetected in the MIR due to the absence or weakness of warm dust emission. MIR surveys conducted with the Midcourse Space Experiment (MSX) and the Infrared Space Observatory (ISO) permitted identification of a large number of Infrared dark Clouds (IRDCs, e.g., Egan et al. 1998). Studies of low-mass IRDCs have constrained the initial conditions of low-mass star formation quite well (e.g., Andre et al. 2000; Bacmann et al. 2000; Alves et al. 2001; Kirk et al. 2005), but the high-mass regime is just beginning to be explored (e.g., Garay et al. 2004; Hill et al. 2005; Klein et al. 2005; Sridharan et al. 2005).

In a 1.2 mm continuum study of High-Mass Protostellar Objects (HMPOs) associated with IRAS sources, we observed serendipitously within the same fields additional mm-peaks not associated with any IRAS source (Beuther et al. 2002a). Correlation of these mm-peaks with the MSX MIR data revealed a sample of mm-peaks that is not only weak in the MIR but seen as absorption shadows against the galactic background (Sridharan et al. 2005). Mass estimates based on the 1.2 mm continuum emission show that they are massive gas cores (of the order a few $100 M_{\odot}$), making them potential High-Mass Starless Core (HMSCs) candidates. Figure 1 shows the HMSC candidate

region IRDC 18223-3 which is a 1.2 mm continuum peak at a distance of ~ 3.7 kpc (Sridharan et al. 2005) in a dust and gas filament approximately $3'$ south of IRAS 18223–1243 (Peak #3 in Beuther et al. 2002a). While the MIR absorption puts the source in the sample of potential HMSCs, a NH_3 rotation temperature of ~ 33 K indicates probable early star formation activity (Sridharan et al. 2005). The region was also identified recently as a massive dense core by Garay et al. (2004).

2. OBSERVATIONS

We observed IRDC 18223-3 with the Plateau de Bure Interferometer (PdBI) during three nights in 2004/2005 at 93 GHz in the C and D configuration covering projected baselines between 15 and 230 m. The 3 mm receivers were tuned to the $\text{N}_2\text{H}^+(1-0)$ line at 93.174 GHz. The phase noise was lower than 30° , and atmospheric phase correction based on the 1.3 mm total power was applied. For continuum measurements we placed two 320 MHz correlator units in the band. The N_2H^+ lines were excluded in averaging the two units to produce the final continuum image. Temporal fluctuations of amplitude and phase were calibrated with frequent observations of the quasars 1741–038 and 1908–201. The amplitude scale was derived from measurements of MWC349. We estimate the final flux accuracy to be correct to within $\sim 15\%$. The phase reference center is R.A.[J2000] $18^{\text{h}}25^{\text{m}}08.3^{\text{s}}$ and Dec.[J2000] $-12^\circ 45' 26.90''$, and the velocity of rest v_{lsr} is 45 km s^{-1} . The synthesized beam of the observations is $5.8'' \times 2.4''$ (P.A. 14°). The 3σ continuum rms is $1.08 \text{ mJy beam}^{-1}$. These mm observations are complemented with the MIR SPITZER data from the GLIMPSE survey of the Galactic plane using the IRAC camera centered at 3.6, 4.5, 5.8 and $8.0 \mu\text{m}$ (Werner et al. 2004; Fazio et al. 2004; Benjamin et al. 2003). Observational details for the CO(2–1) and CS(2–1) observations were given in Sridharan et al. (2002); Beuther et al. (2002a).

¹ Harvard-Smithsonian Center for Astrophysics, 60 Garden Street, Cambridge, MA 02138, USA

² National Astronomical Observatory of Japan, 2-21-1 Osawa, Mitaka, Tokyo, 181-8588, Japan

3. RESULTS AND DISCUSSION

Fig. 2 presents the MIR data toward IRDC 18223-3 as a 3-color composite overlaid with contours of the 93 GHz mm continuum emission. We detect a compact dust and gas core spatially coincident with the MIR dark lane, but we do not detect a (proto)stellar MIR counterpart down to the sensitivity limit of this data (3σ : 0.05 mJy@3.6 μm , 0.05 mJy@4.5 μm , 0.13 mJy@5.8 μm , 0.15 mJy@8.0 μm). The projected size of the mm core in east-west direction is ~ 28000 AU. Assuming the 93 GHz continuum is due to optically thin thermal dust emission, we estimate the mass and column density of the core following Beuther et al. (2002a). Using the temperature of 33 K from NH_3 observations (Sridharan et al. 2005) and a dust opacity index $\beta = 2$, we calculate the mass within the 50% contour level (integrated flux $S_{50\%} \sim 6.7$ mJy) to be $\sim 95 M_\odot$, and the mass within the 3σ level of 1.08 mJy ($S_{3\sigma} \sim 13.0$ mJy) to be $\sim 184 M_\odot$. The peak flux of ~ 5.1 mJy beam $^{-1}$ converts to a peak column density of $\sim 1.0 \times 10^{24}$ cm $^{-2}$, corresponding to a visual extinction of $A_v = N_{\text{H}_2}/0.94 \times 10^{21} \sim 1000$ (Frerking et al. 1982). The uncertainties for mass and column density estimates from dust continuum emission are approximately within a factor 5 (e.g., Beuther et al. 2002a). Single-dish 1.2 mm continuum data (Beuther et al. 2002a) result with the same assumptions in a total mass estimate of $\sim 245 M_\odot$, implying $\sim 25\%$ of missing flux in the PdBI data due to missing short spacings. The data clearly show that we are dealing with a massive gas core at an early evolutionary stage.

While we do not detect a protostellar MIR source toward the mm-peak IRDC 18223-3, Fig. 2 shows weak emission in the SPITZER 4.5 μm band (IRAC band 2 color-coded in green) toward the south-east, the north-west and at the western edge of the mm core. These features are just detected in the IRAC band 2. Since a foreground source would also show up at 3.6 μm , and an embedded protostellar object would be red and thus also detectable at 5.8 and 8.0 μm if PAH features are not too bright, these 4.5 μm features are unlikely to be of (proto)stellar nature. One cannot entirely exclude that the 4.5 μm emission is due to highly reddened background sources (e.g., the MIR lower limit magnitudes imply minimum visual extinctions $A_v > 40$ and $A_v > 120$ for the south-eastern and the western 4.5 μm features, respectively.), but it is more likely that the 4.5 μm features are due to line emission within the IRAC band 2 bandpass (approximately 4 to 5 μm). SPITZER outflow observations showed that molecular outflows are particularly strong in the 4.5 μm band because of H_2 and CO line emission (e.g., Noriega-Crespo et al. 2004). Hence, we suggest that the 4.5 μm emission at the edge of the mm core may be due to shock excitation as the outflow collides with the ambient molecular medium. The two 4.5 μm features to the south-east and north-west are on opposite sides of the main mm-peak which is indicative of typical bipolar outflows (Richer et al. 2000). The additional third feature to the west is suggestive of multiple outflows as often observed in massive star-forming regions (e.g., Beuther et al. 2003).

Support for this outflow interpretation is provided by single-dish CO(2–1) and CS(2–1) observations from the Caltech Submillimeter Observatory (CSO) and the IRAM 30m telescope (Sridharan et al. 2002; Beuther et al.

2002a). Both spectra presented in Fig. 3 show line-wing emission in excess of a Gaussian line component at the $v_{\text{lsr}} \sim 45$ km s $^{-1}$. The Full Width at Zero Intensity of both lines is ~ 24 km s $^{-1}$. The CO(2–1) spectrum shows two additional line components at ~ 51 and ~ 62 km s $^{-1}$. Comparing these features with CO(2–1) spectra toward other positions of the large-scale dust filament (Fig. 1), the 51 km s $^{-1}$ component is also present toward the rest of the filament whereas the 62 km s $^{-1}$ component is observed only toward IRDC 18223-3. This difference indicates that the 52 km s $^{-1}$ component is probably part of a larger-scale foreground or background cloud, whereas the 62 km s $^{-1}$ component is likely due to the molecular outflow. Following Beuther et al. (2002b), we roughly estimate the mass of high-velocity gas within the CSO primary beam (31'') to be $\sim 3.4 M_\odot$. Compared to other typical high-mass outflows (e.g., Beuther et al. 2002b), this is a relatively low value. However, since we are presumably dealing with a source at the onset of massive star formation, there has not been much time yet to eject and entrain molecular gas, and thus comparably low outflow masses are expected at this evolutionary stage.

In addition, we observed the $\text{N}_2\text{H}^+(1-0)$ line with seven hyperfine components around 93.174 GHz (Fig. 3), which is known to be strong and optically thin in low-mass starless cores (Tafalla et al. 2004). Fig. 4 presents the $\text{N}_2\text{H}^+(1-0)$ emission integrated over all hyperfine components, and over a smaller velocity interval centered on the isolated $\text{N}_2\text{H}^+(1-0)$ component at 93176.27 MHz. Both N_2H^+ maps show an emission peak toward the main IRDC 18223-3 mm continuum peak. Moreover, the N_2H^+ data exhibit a secondary peak $\sim 7''$ to the east of this main peak, spatially associated with the MIR absorption north-east of the 4.5 μm emission. Furthermore, we find that the N_2H^+ line-width Δv increases from the outer edges of the N_2H^+ emission in the direction toward the main IRDC 18223-3 mm-peak (Fig. 4). Although the main IRDC 18223-3 peak likely exhibits multiple velocity components (see below), the general trend of increasing Δv appears real. This is indicative of increased internal motion within the main IRDC 18223-3 core – either turbulent or ordered motion like infall, rotation or outflow. We interpret this as additional evidence for the onset of star formation activity. The line-width is still narrow toward the IRDC 18223-3 secondary N_2H^+ peak with $\Delta v \sim 1$ km s $^{-1}$, indicating less internal motion and hence likely an earlier evolutionary stage.

Fitting the N_2H^+ hyperfine structure permits determination of the optical depth and N_2H^+ column density (e.g., Caselli et al. 2002b). Unfortunately, we cannot derive a good fit toward the main IRDC 18223-3 mm-peak because the N_2H^+ spectrum shows excess emission 1-2 km s $^{-1}$ offset from the peak velocity (Fig. 3) indicative of multiple velocity components. The spectral fitting difficulties are likely due to this complex velocity structure. In contrast, we can fit the spectrum toward the secondary IRDC 18223-3 N_2H^+ peak reasonably well (Fig. 3). The resulting N_2H^+ column density of 3.1×10^{13} cm $^{-2}$ translates into an H_2 column density of $N_{\text{H}_2} \sim 1.0 \times 10^{23}$ cm $^{-2}$, assuming a $\text{N}_2\text{H}^+/\text{H}_2$ ratio of 3×10^{-10} (Caselli et al. 2002a). Since the 3 mm continuum 3σ rms of 1.08 mJy corresponds to an H_2 column density sensitivity between 2.2×10^{23} and

$5.2 \times 10^{23} \text{ cm}^{-2}$ (assuming 33 and 15 K, respectively), the continuum non-detection of this N_2H^+ secondary peak is a plausible observational result. Assuming a lower temperature of 15 K (typical for HMSC candidates, Sridharan et al. 2005), the 3σ mm continuum sensitivity implies that a core as massive as $37 M_\odot$ can be hidden toward this secondary N_2H^+ peak without being detected in our mm continuum data.

We estimate the virial masses of the IRDC 18223-3 main and secondary N_2H^+ peaks for the observed line-widths Δv (2.0 and 1.0 km s^{-1} , Fig. 4) and sizes R ($\sim 14000 \text{ AU}$ for both peaks) following MacLaren et al. (1988). Assuming different density distributions ($\rho \propto 1/r$ & $\rho \propto 1/r^2$), the derived virial masses are 51 & 34 and 13 & $8 M_\odot$ for the two N_2H^+ peaks, respectively. This estimate for the main N_2H^+ peak is more than a factor 3 lower than what we derived from the 93 GHz mm continuum emission. Although the error budget is high for the various mass estimates (about a factor 5, Beuther et al. 2002a), the smaller virial mass compared to the gas mass derived from the mm continuum is consistent with this core collapsing to form a star. The virial mass of the secondary N_2H^+ peak is consistent with the previously derived upper mass limits from the mm continuum. Hence, the secondary core may still be in a virially bound state, potentially prior to active star formation.

In summary, the observational features of (i) a massive IRDC, (ii) a molecular outflow as suggested by the $4.5 \mu\text{m}$, CO and CS emission, (iii) the N_2H^+ line-width and virial analysis, and (iv) the high NH_3 temperatures indicate the presence of an extremely young massive protostellar object at the center of the mm continuum core IRDC 18223-3, which remains otherwise undetected in the MIR due to its extreme youth and the high gas column densities. Although this line of evidence is still circumstantial and has to be further investigated, the MIR non-detection and the comparably low outflow mass supports an early evolutionary stage prior to the typically studied HMPOs. The narrow linewidth and associated virial mass of the lower-mass secondary N_2H^+ peak suggests that it may be in an even younger pre-protostellar stage prior to any active star formation.

IRAM is supported by INSU/CNRS (France), MPG (Germany), and IGN (Spain). SPITZER is operated by the JPL, Caltech under NASA contract 1407. We wish to thank J. Hora, C. de Vries, J. Joergensen, T. Bourke, T. Megeath and T. Huard for help with the SPITZER and N_2H^+ data. We also thank the referee for detailed comments improving the paper. H.B. acknowledges financial support by the Emmy-Noether-Programm of the Deutsche Forschungsgemeinschaft (DFG, grant BE2578).

REFERENCES

- Alves, J. F., Lada, C. J., & Lada, E. A. 2001, *Nature*, 409, 159
- Andre, P., Ward-Thompson, D., & Barsony, M. 2000, *Protostars and Planets IV*, 59
- Bacmann, A., André, P., Puget, J.-L., et al. 2000, *A&A*, 361, 555
- Benjamin, R. A., Churchwell, E., Babler, B. L., et al. 2003, *PASP*, 115, 953
- Beuther, H., Schilke, P., Menten, K. M., et al. 2002a, *ApJ*, 566, 945
- Beuther, H., Schilke, P., Sridharan, T. K., et al. 2002b, *A&A*, 383, 892
- Beuther, H., Schilke, P., & Stanke, T. 2003, *A&A*, 408, 601
- Caselli, P., Benson, P. J., Myers, P. C., & Tafalla, M. 2002a, *ApJ*, 572, 238
- Caselli, P., Walmsley, C. M., Zucconi, A., et al. 2002b, *ApJ*, 565, 344
- Churchwell, E. 2002, *ARA&A*, 40, 27
- Egan, M. P., Shipman, R. F., Price, S. D., et al. 1998, *ApJ*, 494, L199
- Fazio, G. G., Hora, J. L., Allen, L. E., et al. 2004, *ApJS*, 154, 10
- Frerking, M. A., Langer, W. D., & Wilson, R. W. 1982, *ApJ*, 262, 590
- Garay, G., Faúndez, S., Mardones, D., et al. 2004, *ApJ*, 610, 313
- Hill, T., Burton, M., Minier, V., et al. 2005, *MNRAS* accepted, astro-ph/0506402
- Kirk, J. M., Ward-Thompson, D., & André, P. 2005, *MNRAS*, 360, 1506
- Klein, R., Posselt, B., Schreyer, K., Forbrich, J., & Henning, T. 2005, *ArXiv Astrophysics e-prints* astro-ph/0508191
- Kurtz, S., Cesaroni, R., Churchwell, E., Hofner, P., & Walmsley, C. M. 2000, *Protostars and Planets IV*, 299
- MacLaren, I., Richardson, K. M., & Wolfendale, A. W. 1988, *ApJ*, 333, 821
- Molinari, S., Brand, J., Cesaroni, R., & Palla, F. 1996, *A&A*, 308, 573
- Noriega-Crespo, A., Morris, P., Marleau, F. R., et al. 2004, *ApJS*, 154, 352
- Richer, J. S., Shepherd, D. S., Cabrit, S., Bachiller, R., & Churchwell, E. 2000, *Protostars and Planets IV*, 867
- Sridharan, T. K., Beuther, H., Saito, M., Wyrowski, F., & Schilke, P. 2005, *ApJ* submitted
- Sridharan, T. K., Beuther, H., Schilke, P., Menten, K. M., & Wyrowski, F. 2002, *ApJ*, 566, 931
- Tafalla, M., Myers, P. C., Caselli, P., & Walmsley, C. M. 2004, *A&A*, 416, 191
- Werner, M. W., Roellig, T. L., Low, F. J., et al. 2004, *ApJS*, 154, 1

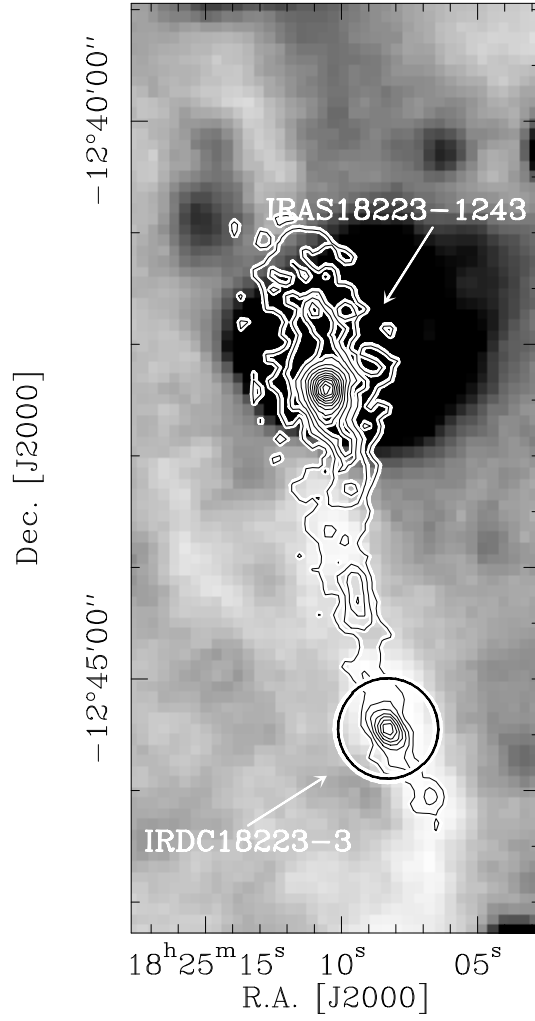


FIG. 1.— Contour overlay of the 1.2 mm single-dish continuum map Beuther et al. (2002a) on the $8\ \mu\text{m}$ MSX image (in grey-scale). The contour levels are from 38 mJy in 38 mJy steps. The northern source is the High-Mass Protostellar Object (HMPO) IRAS 18223-1243, and the southern source is the High-Mass Starless Core candidate IRDC 18223-3. The black circle outlines the primary beam of the Plateau de Bure Interferometer observations.

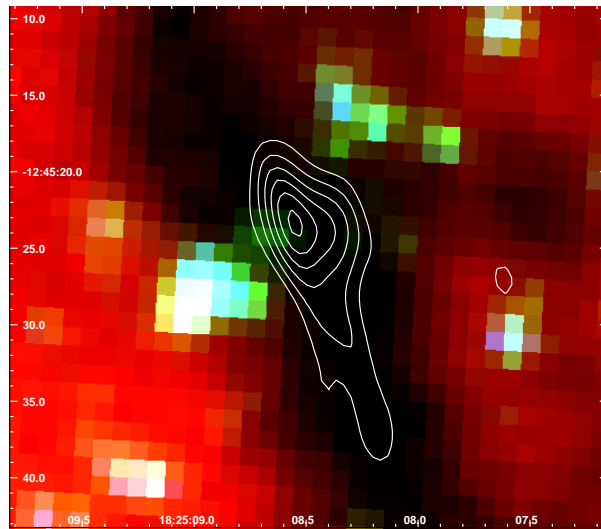


FIG. 2.— Three color image of the SPITZER IRAC observations at 3.6 (blue), 4.5 (green) and 8.0 μm (red). The contours show the PdBI 93 GHz continuum map from 1.08 mJy (3σ) in 0.72 mJy steps (2σ). The axis are in R.A. [J2000] and Dec. [J2000].

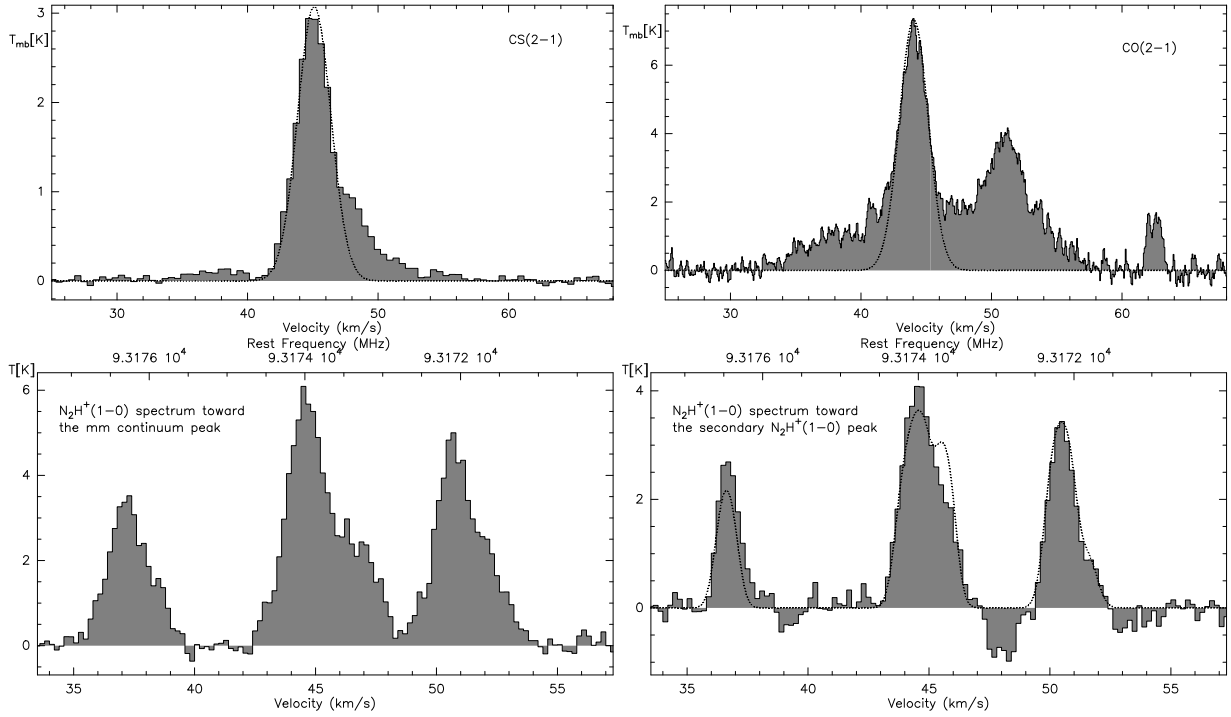


FIG. 3.— **Top:** Single-dish CS(2–1) and CO(2–1) spectra toward IRDC 18223-3 observed with the IRAM 30 m and CSO, respectively. The solid lines show the spectra and the dotted lines Gaussian fits to the central line component at $v_{LSR} \sim 45 \text{ km s}^{-1}$. Obviously, both spectra show strong excess line wing emission indicative of a high-velocity molecular outflow. **Bottom:** $N_2H^+(1-0)$ spectra in IRDC 18223-3 toward the 93 GHz continuum peak (left) and the secondary $N_2H^+(1-0)$ peak $\sim 7''$ to the east (right) observed with the PdBI. Note that the presented velocity range is smaller than for the CO/CS spectra. The N_2H^+ spectra cover all seven hyperfine components, the rest-frequency is set to the hyperfine group frequency of 93173.770 MHz. The dotted line in the right spectrum shows the fit to the hyperfine structure. The negative features in the right spectrum are not real absorption features but due to the negative side-lobes caused by the missing short spacing data in the corresponding velocity channels toward this position.

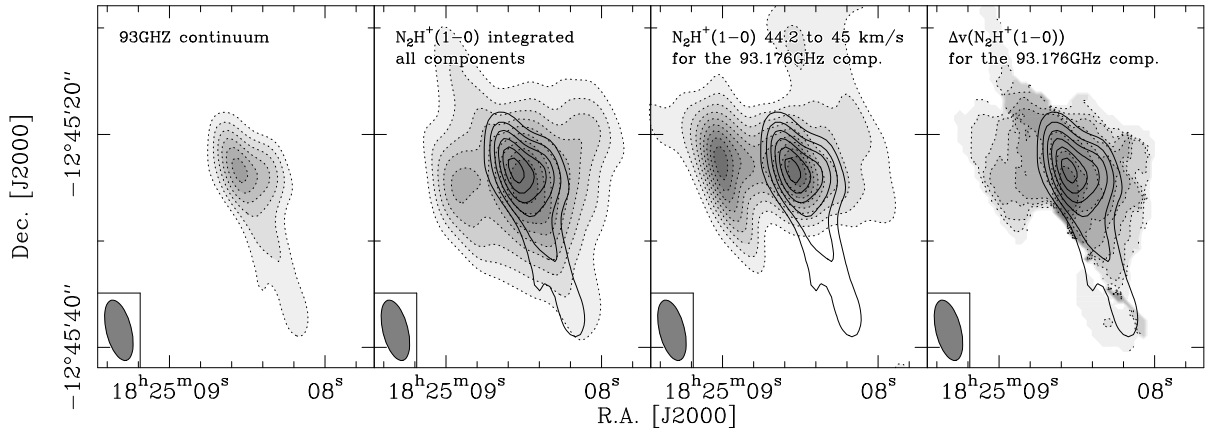


FIG. 4.— 93 GHz continuum and $\text{N}_2\text{H}^+(1-0)$ emission and line-width maps toward IRDC 18223-3. The grey-scale with thin dotted contours shows the 93 GHz continuum and $\text{N}_2\text{H}^+(1-0)$ maps as labeled within each panel. The solid contours in panels 2 to 4 again show the 93 GHz continuum emission. The contouring of the continuum starts at 1.08 mJy (3σ) and proceeds in 0.72 mJy steps (2σ). The contour levels of the $\text{N}_2\text{H}^+(1-0)$ maps range always from 10 to 90 % of the peak values ($23.5 \text{ Jy beam}^{-1}$, 1.2 Jy beam^{-1} and 2.0 km s^{-1} , respectively). The synthesized beam is shown at the bottom-left of each panel.